Latitudinal Variations Observed in Gravity Waves with Short Vertical Wavelengths

M. JOAN ALEXANDER

Colorado Research Associates Division, NorthWest Research Associates, Inc., Boulder, Colorado

TOSHITAKA TSUDA

Radio Science Center for Space and Atmosphere, Kyoto University, Kyoto, Japan

ROBERT A. VINCENT

Department of Physics and Mathematical Physics, University of Adelaide, South Australia, Australia

(Manuscript received 18 October 2000, in final form 17 August 2001)

ABSTRACT

Knowledge of the latitudinal variations in the occurrence of gravity waves is important for their parameterization in global models. Observations of gravity waves with short vertical scales have shown a pronounced peak in wave activity at tropical latitudes. In this paper, it is shown that such a peak may be a natural consequence of the latitudinal variation in the Coriolis parameter, which controls the lower limit for gravity-wave intrinsic frequencies $\hat{\omega}$. Two distinct but related effects of this parameter on observations of gravity-wave activity are explained and explored with a simple model. The results are also compared to observed latitudinal variations in gravity-wave activity. The authors formally distinguish between observed gravity-wave spectra and what is called gravity-wave ''source spectra,'' the latter being appropriate for input to gravity-wave parameterizations. The results suggest that the $\hat{\omega}^{-5/3}$ dependence of the gravity-wave energy spectrum commonly assumed as input to parameterizations is likely too steeply sloped. Much more shallowly sloped spectra for gravity-wave parameterization input $\propto \hat{\omega}^{-0.6} - \hat{\omega}^{-0.7}$ show better agreement with observations. The results also underscore the potential importance of intermittency in gravity-wave sources to the interpretation of gravity-wave observations.

1. Introduction

Several recent studies have derived geographical variations in gravity-wave activity from observations in the lower stratosphere. Tsuda et al. (2000) used data from the Global Positioning System (GPS) Meteorology (GPS/MET) project, Allen and Vincent (1995) and Hirota (1984) analyzed observations from high-resolution radiosondes, Eckermann et al. (1995) analyzed rocket measurements, Fetzer and Gille (1994) used data from the Limb Infrared Monitor of the Stratosphere (LIMS) satellite data, Wu and Waters (1996) and McLandress et al. (2000) used Microwave Limb Sounder (MLS) satellite data, and Eckermann and Preusse (1999) show results from Cryogenic Infrared Spectrometers and Telescopes for the Atmosphere (CRISTA). Such observed variations provide potentially useful constraints for gravity-wave parameterizations that must specify gravity-wave sources somewhere in the lower atmosphere in global models. How these sources vary remains an enormous source of uncertainty in the application of these parameterizations (e.g., Rind et al. 1988; Kinnersley 1996; Medvedev et al. 1998; Manzini and McFarlane 1998; Alexander and Dunkerton 1999). Ideally, our knowledge of wave sources and our understanding of the mechanisms for wave generation would be complete enough that parameterized gravity waves could be specified with realistic properties at appropriate times and locations according to these sources. Currently only topographic wave sources are parameterized this way with moderate success. State of the art global models that try to include parameterized gravity waves from other sources specify some simple latitudinally varying distribution of gravity waves at an arbitrary level in the troposphere or lower stratosphere (Scaife et al. 2000; Manzini and McFarlane 1998; Medvedev et al. 1998).

Although it is hoped that global variations observed in gravity waves can be used to constrain these parameterizations, the interpretation of these variations must first be considered carefully (Eckermann 1995; Alexander 1998). Because each observation method has a unique set of capabilities and limitations, and because gravity wave properties cover a very broad range, each observation method will only detect some fraction of

Corresponding author address: Dr. M. Joan Alexander, NorthWest Research Associates, Inc., 3380 Mitchell Lane, Boulder, CO 80301.
E-mail: alexand@colorado-research.com

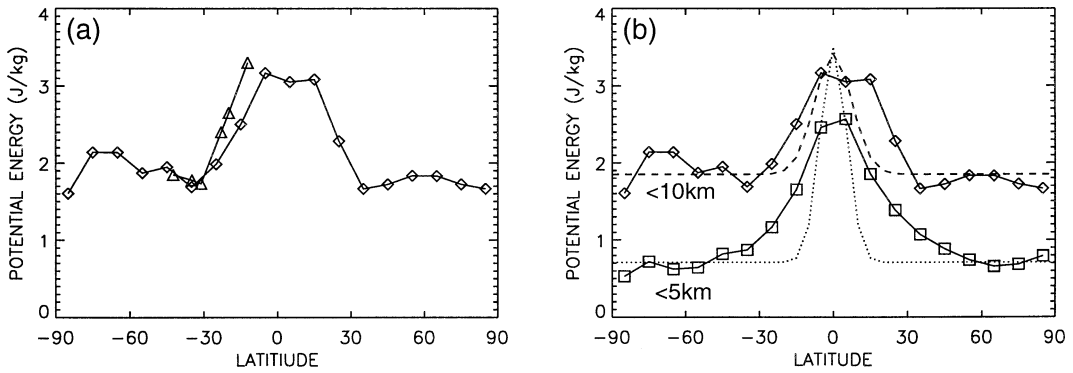

FIG. 1. Observations of gravity-wave potential energy vs latitude averaged over 18–25-km altitudes in the lower stratosphere. (a) Diamonds show GPS/MET observations (Tsuda et al. 2000) filtered to include vertical wavelengths 1.5–10 km and averaged over all the available data, including months May through Feb. Triangles show Australian radiosonde data (Allen and Vincent 1995) averaged over a full year. The radiosondes include vertical wavelengths 0.75–7 km. (b) Diamonds are the same as in (a) and squares show the same GPS/MET data filtered to include vertical wavelengths 1.5–5 km. The dashed and dotted curves represent theoretical potential energy for Kelvin waves with 10- and 5-km vertical wavelengths, respectively. These represent the Kelvin wave energy superimposed on a background level of contstant gravity-wave activity with latitude.

the waves that may be occurring. Alexander (1998) referred to these limitations as ''observational filters.'' Fairly simple models can be used to quantify the effects of observational filters in order to aid in the interpretation of patterns observed in gravity-wave activity. Recent studies employing these methods include Eckermann and Preusse (1999) for interpreting a CRISTA mountain wave event, McLandress et al. (2000) for interpretation of geographical variations in the MLS gravity-wave observations, Alexander and Vincent (2000) for interpretation of seasonal and interannual variations in gravity waves appearing in tropical radiosonde profiles, and Preusse et al. (2000) for use in a comparison study of different satellite observations.

Gravity wave temperature variance derived from both GPS (Tsuda et al. 2000) and radiosonde (Allen and Vincent 1995) observations show peaks at low latitudes when averaged over annual or seasonal timescales (see Fig. 1). These data were analyzed by subtracting a smoothly varying background vertical profile then assuming that the remaining fluctuations were gravity waves. This procedure applies a high-pass observational filter on the vertical wavenumber spectrum of the waves that may be present. (There is also a limit on the shortest observable vertical wavelengths related to the vertical resolution.) Previous analyses of radiosonde and rocket profiles have demonstrated that these short vertical scale fluctuations display properties of low intrinsic frequency $\hat{\omega}$ inertia–gravity waves (Hirota 1984; Hamilton 1991; Eckermann et al. 1995; Vincent et al. 1997; Vincent and Alexander 2000; Alexander and Vincent 2000). It will be shown below that observations like these that include low-frequency waves can be expected to show a peak in gravity-wave activity at the equator. Other examples are observations from the LIMS satellite (Fetzer and Gille 1994, 1996) and the Space Shuttle CRISTA experiment (Eckermann and Preusse 1999; Preusse et al. 2000).

Some of these studies have also inferred a preference toward eastward propagation of these waves leading to the suggestion that the equatorial maximum in potential energy E_p may be due to short vertical-wavelength Kelvin wave modes (Eckermann 1995). Indeed, Kelvin waves with vertical wavelengths as short as 3 km have been observed at the equator (Holton et al. 2001). However, Kelvin wave variance has a predictable latitudinal width that varies in proportion to the vertical wavelength. It will be shown in section 2 that this width is much narrower than the equatorial peak in Fig. 1.

We present two perspectives on the interpretation of the observed latitudinal variations in gravity-wave energy. Both perspectives will be shown to imply that these observations are dominated by the lowest intrinsic frequency gravity waves, and that the occurrence of a low-latitude peak is directly related to the variation in the Coriolis parameter with latitude. An issue that we try to emphasize here is that observed spectra of gravity wave energy do not directly provide the constraints needed to parameterize gravity wave effects in global models. Parameterizations that rely on local instability theory to describe wave dissipation (e.g., Lindzen 1981; McFarlane 1987; Warner and McIntyre 2001; Hines 1997; Alexander and Dunkerton 1999) need as input a distribution of gravity wave amplitudes at some reference level (or source level). If there is intermittency in wave forcing, these wave amplitudes will differ from the temporally and/or spatially averaged amplitudes that result from spectral analysis. In addition, monthly or seasonal means of wave activity are commonly reported. Studies such as Ecklund et al. (1986) and Sato (1990) underscored the potential importance of intermittency

for high-frequency waves that dominate vertical velocity observations.

The theoretical ideas presented here illustrate how differences between an intermittently forced wave spectrum and a continuously forced spectrum can be important. The framework employed is, however, highly simplified: effects of shear (e.g., Fritts and VanZandt 1987) are neglected here. However, for the time-mean observations in the lowermost stratosphere to which we compare our theoretical results, shear effects are minimized. The wave sources are further treated as unvarying in latitude, an assumption applied partly for the purpose of isolating the effects of the Coriolis parameter and also for lack of a more complete understanding of wave sources.

Section 2 describes the observations in more detail, and section 3 presents the basic theoretical ideas and resulting calculations for comparison to the observations. A summary and discussion follow (section 4), and brief conclusions appear in section 5.

2. Observed latitudinal variations in short vertical-wavelength waves

Figure 1a shows latitudinal variations in gravity-wave potential energy E_p derived from temperature perturbation measurements in the lower stratosphere from the GPS/MET satellite observations (Tsuda et al. 2000) and from Australian radiosonde observations (Allen and Vincent 1995) for altitudes in the lower stratosphere, 18–25 km. The GPS/MET observations include waves with vertical wavelengths 1.5–10 km, and these data include only the months May through February with no data in the Southern Hemisphere late-summer-to-fall season. These missing months and the annual migration of intertropical convergence zone (ITCZ) convection across the equator may explain why the peak is not centered on the equator but shifted toward the north. The radiosonde observations represent a full year of data but only at a limited range of latitudes and longitudes near Australia.

The observations show large increases in gravity-wave activity at low latitudes. The ratio of low-latitude (5°) to higher-latitude (35°) potential energy is 1.9 averaged over all seasons of the GPS observations (diamonds in Fig. 1b). Substantially more activity begins to appear at latitudes equatorward of 30°. This is one indication that the low-latitude peak is not solely due to contamination by equatorial planetary-scale waves, which would be confined much more closely to the equator (Andrews et al. 1987). Another indication is that the peak persists after filtering waves with vertical wavelengths >5 km from the data (squares in Fig. 1b), a procedure that should eliminate the dominant planetary-scale wave perturbations (Andrews et al. 1987). The dashed and dotted lines plotted in Fig. 1b show potential energies for Kelvin waves with vertical wavelengths of 10 and 5 km, respectively. The β-plane approximation to the latitudinal variation of Kelvin wave energy has the form $\exp(-|m|f^2/\beta N)$, where m is the vertical wavenumber, $\beta = 2\Omega/a$ ($\Omega = 7.292 \times 10^{-5}$ s^{-1}, the earth's rotation rate; and $a = 6378$ km, earth's equatorial radius), $f = 2\Omega \sin\phi \sim \beta a\phi$ is the Coriolis parameter (ϕ = latitude), and $N = 0.02$ s^{-1}, buoyancy frequency. The Kelvin wave energy is normalized in Fig. 1b to equal the observed E_p at 5° latitude to illustrate that even if all of the observed signal at that latitude were due to Kelvin waves, such waves cannot explain the increase that appears equatorward of 30° latitude. Note also that equatorially trapped planetary-scale Rossby–gravity and inertia–gravity waves have the same latitudinal decay scale in amplitude as that shown for Kelvin waves (Fig. 1b).

Further evidence that the low-latitude peak in these data is associated primarily with inertia–gravity waves comes from analyses of radiosonde data similar to these but that included horizontal wind vector measurements (Kitamura and Hirota 1989; Tsuda et al. 1994; Ogino et al. 1995; Vincent and Alexander 2000). These data have clearly shown elliptical polarization relationships between the horizontal wind components that are the signature of inertia–gravity waves, those with $\hat{\omega} \sim f$. Such observations have also shown a ratio of kinetic to potential energies >1 (Vincent and Alexander 2000), consistent with low-frequency gravity waves. The radiosonde observations (triangles in Fig. 1a) only cover latitudes 12° and higher, but a clear increase at lower latitudes is obvious even there. The ratio of potential energy at 12° to that at 35° is 1.9 in these data.

For the remainder of this paper, the waves in the observations in Fig. 1 will be assumed to be internal gravity waves satisfying the dispersion relation,

$$\hat{\omega}^2 = \frac{N^2k^2 + f^2m^2}{k^2 + m^2}. \quad (1)$$

We again note that the observations closest to the equator could still include contamination from some Kelvin wave modes or from equatorially trapped inertia-gravity wave modes. The latter have a different dispersion relationship and group velocity dependence on frequency than treated here. Such differences would affect the calculations in sections 3b and 3c. These waves alone, however, cannot explain the existence of the low-latitude peak seen in the observations because their latitudinal widths are much narrower than the observed peak.

The data in Fig. 1 therefore show that short vertical wavelength gravity wave potential energy increases from mid- to low latitudes by a factor ~2. We next explore some effects that may account for this low-latitude energy peak.

3. Latitudinal variations in low-frequency gravity waves

The Coriolis parameter f sets the low intrinsic frequency $\hat{\omega}$ limit for gravity waves. Vertical shear in the

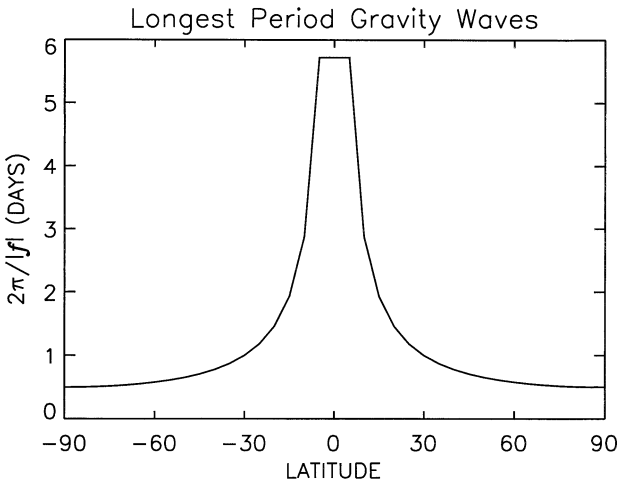

FIG. 2. Variation of the longest-allowed period for gravity waves as a function of latitude.

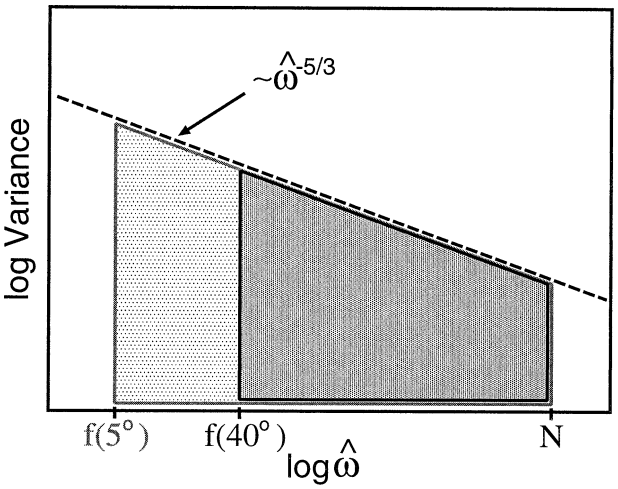

FIG. 3. Illustration of latitudinal variations associated with a red variance spectrum $\propto\hat{\omega}^{-5/3}$. The dark gray area represents the integral over the gravity-wave spectrum at 40° latitude. The light gray area represents the additional contribution to the integral closer to the equator at 5° latitude.

background wind can shift $\hat{\omega}$ as the wave propagates vertically through the atmosphere, but in the limit $|\hat{\omega}| \rightarrow |f|$, the wave's vertical wavelength λ_z and vertical group velocity c_{gz} both $\rightarrow 0$. This level is a critical level for the wave, and dissipation or instability would likely obliterate the wave perturbations near or below this level.

The longest gravity-wave period $2\pi/|f|$ (Fig. 2) varies with latitude because of the variation in the Coriolis parameter f. This theoretical limit on gravity-wave period actually increases to infinity at the equator, but only latitudes poleward of 5° are plotted.

The equatorial peak that appears in Fig. 2 could lead to a peak in gravity-wave temperature variance in any set of measurements sensitive to low-frequency waves via two effects.

1) If the forcing for gravity waves generates an intrinsic frequency spectrum that is "red" (i.e., the temperature spectrum varies as $\hat{\omega}^{-p}$ where $p > 0$), then as the maximum allowed period for gravity waves becomes longer near the equator, the wave variance near the equator would increase.
2) The vertical group velocity of gravity waves decreases with decreasing $\hat{\omega}$. As the minimum allowed $\hat{\omega}$ decreases near the equator, the lowest-frequency waves will take longer and longer to propagate through the altitude region in the stratosphere where they are observed. If there is intermittency in the forcing of these waves, such as might be expected if convection were the source, then the probability of observing the waves increases at the equator also. Gravity-wave activity averaged over some longer timescale, such as a month, would then peak at the equator as well.

The second group velocity effect described in effect 2 above was noted by Thompson (1978) in reference to inertia–gravity waves in radiosonde observations. We will develop a simple theoretical model for exploring these effects that will help to relate the observations to constraints that are needed as input to gravity wave parameterizations. Exploring and quantifying the effects of the two hypothesized mechanisms above is the subject of the present paper. The results will be compared to observations and used to aid in the interpretation of the observed latitudinal variations in gravity-wave sources.

a. Effects of a wave spectrum $\propto\hat{\omega}^{-p}$

Figure 3 illustrates how a red energy spectrum could contribute to latitudinal variations in observed gravity-wave variance. Assuming the observed potential energy E_p represents an integral over the spectrum $E_o(\hat{\omega})$ from the inertial frequency f to the buoyancy frequency N,

$$E_p(\phi) = \int_{f(\phi)}^{N} E_o(\hat{\omega})\, d\hat{\omega}, \tag{2}$$

will be a function of latitude. The integral can be evaluated analytically for forms $E_o = B\hat{\omega}^{-p}$ such that

$$E_p(\phi) = \begin{cases} B(N^{1-p} - |f(\phi)|^{1-p})/(1-p) & \text{for } p \neq 1 \\ B(\ln|N/f(\phi)|) & \text{for } p = 1. \end{cases} \tag{3}$$

Observations do not generally quantify the intrinsic frequency $\hat{\omega}$ spectrum of gravity waves. Instead, the gravity-wave frequency spectrum relative to the ground ω is most commonly observed. For a linear gravity wave with horizontal wavenumber k,

$$\hat{\omega} = \omega - \overline{u}k, \tag{4}$$

where $\overline{u}$ is the background wind speed in the direction

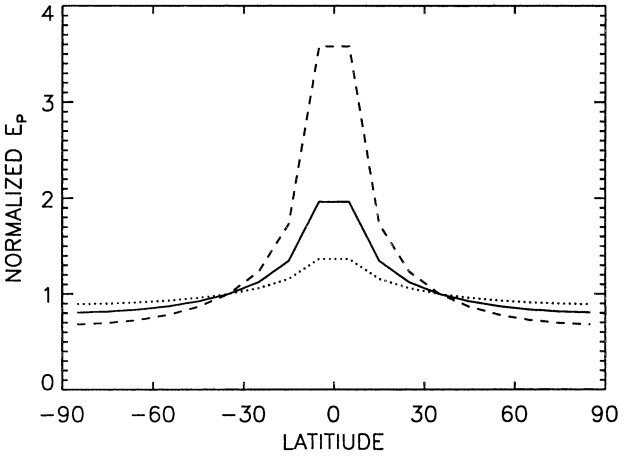

FIG. 4. Latitudinal variations in normalized variance assuming no intermittency in the wave sources and a source spectrum proportional to $\hat{\omega}^{-p}$ where $p = 5/3$ (dashed), $p = 1.3$ (solid), $p = 1$ (dotted). These curves demonstrate the effects of effect 1.

of wave propagation. Observations of gravity wave horizontal wind and temperature spectra vary approximately $\propto\omega^{-5/3}$ (Fritts and VanZandt 1993). Warner and McIntyre (1996) have proposed that an intrinsic frequency spectrum $\propto\hat{\omega}^{-1}$ near the tropopause gives a better fit to mesospheric observations than $\hat{\omega}^{-5/3}$. Quinn and Holzworth (1987) reported quasi-Lagrangian density spectra obtained from balloons at 26-km altitude. These suggest an intrinsic frequency spectrum $\sim\hat{\omega}^{-5/3}$ for short period waves $\leq$3 h at $\sim$45°S. Hertzog and Vial (2001) also show vertical wind spectra from similar balloon flights at equatorial latitudes. From these, a potential energy spectrum $\sim\hat{\omega}^{-2}$ is inferred for short-period waves and a much flatter spectrum for longer-period waves. Note that the mechanism illustrated in Fig. 3 would suggest that only rather long-period gravity waves, primarily those with frequencies lower than high-latitude values of f, would be the ones responsible for most of the latitudinal variation in E_p. These existing constraints therefore still permit a wide range in the shape of the $\hat{\omega}$ spectrum at low frequencies, so we vary it here as $\hat{\omega}^{-p}$ with $5/3 \geq p \geq 1$ to illustrate a range of effects.

Figure 4 shows the function $E_p(\phi)$ for three values of p. Each curve has been normalized to unity at $\phi = 35°$. At $p = 1$, E_p varies only very weakly with latitude. As p increases, however, dramatic increases in the Tropics appear. In the GPS observations (Tsuda et al. 2000), the ratio of variance $E_p(5°)/E_p(35°) \sim 1.9$, so a value $p \sim 1.3$ for low-frequency waves would be implied by this simple model to best fit the observations. By low frequency, we mean waves with periods longer than $\sim$12–20 h.

If gravity waves were forced continuously at all frequencies, then an equation like (3) could represent observations. The value of $p = 1.3$ seems low in light of radar and radiosonde data (Fritts et al. 1990; Shimizu and Tsuda 1997) that indicate energy spectra proportional to $\omega^{-5/3}$, and the balloon data cited above indicate steeper intrinsic frequency spectra as well, particularly at shorter periods less than 1 day. If there is intermittency in the forcing of gravity waves, however, as would be expected for tropical convectively generated gravity waves, then the group velocity effects in effect 2 could also be important. These group velocity effects will tend to steepen the observed spectrum over a wide range of intrinsic frequencies. These effects are explored in the next section.

b. Group velocity effects with intermittent wave sources

In linear theory, the vertical group velocity c_{gz} of a gravity wave is,

$$c_{gz} = \frac{-(\hat{\omega}^2 - f^2)}{\hat{\omega}m\left(1 + \dfrac{\hat{\omega}^2 - f^2}{N^2 - \hat{\omega}^2}\right)}, \tag{5}$$

where m is the vertical wavenumber. For upward propagating gravity waves, $\hat{\omega}m < 0$ and $c_{gz} > 0$. Assuming there is some spatial and temporal intermittency in gravity-wave forcing, then waves of different frequency would be expected to propagate at different speeds across the altitude layer in which they can be observed. Intermittent wave packets have been seen in radar (Sato et al. 1997) and radiosonde (Pfister et al. 1986; Zink and Vincent 2001) observations in the lower stratosphere.

To quantify this effect, we assume a packet can be described by some discrete $\hat{\omega}$ and m (e.g., associated with a central value or spectral peak). Then neglecting vertical shear, the time τ it will take for the packet to travel across the height region Δz in which it can be observed is given by

$$\tau = \frac{\Delta z}{c_{gz}}. \tag{6}$$

For comparison to the data plotted in Fig. 1, Δz will be 7 km.

Let ϵ_0 represent the fractional area of the observed region that the wave packet covers. For the zonal-mean GPS observations, for example, ϵ_0 would be the ratio of the areal footprints of wave packets divided by the area of a 10° wide latitude band. Let t_1 be the duration of the wave forcing and t_2 be the time interval between forcing periods. If we then treat the wave packet as a thin pancake, as if the packet depth $\ll\Delta z$ (or $t_2 \gg t_1$), then the probability P of observing the packet is

$$P = \frac{\epsilon_0}{t_2}\frac{\Delta z}{c_{gz}(\hat{\omega})} \leq 1. \tag{7}$$

Note the additional constraint that the probability of observing the wave cannot exceed unity.

Figure 5 shows examples of the dependence of this

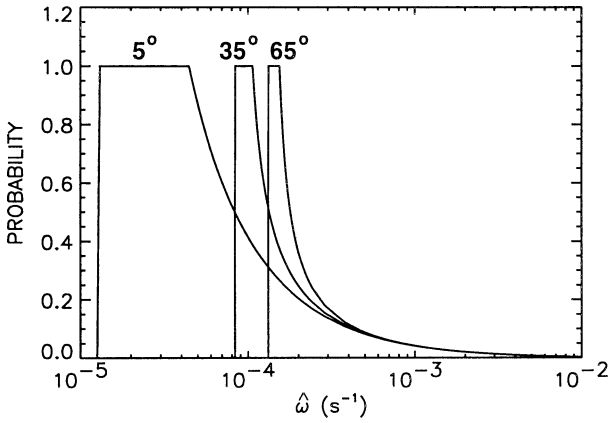

FIG. 5. Curves showing probability of observation as a function of wave intrinsic frequency at three different latitudes: 5°, 35°, and 65°. For each curve, a vertical wavelength of 2.5 km, and a source intermittency of 1 day has been assumed. The probability is very low at high $\hat{\omega}$ because of the very fast vertical group velocities of these waves. The probability then climbs steeply toward 1 as $\hat{\omega}$ approaches f. The curves go immediately to zero at $\hat{\omega} = f$, the gravity wave low-frequency limit.

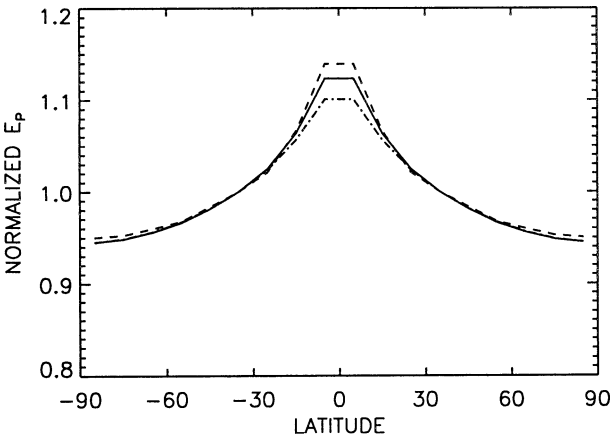

FIG. 6. Latitudinal variations in normalized potential energy due to the probability effect associated with the group velocity dependence on $\hat{\omega}$. Wave source intermittency periods t_2 of 5 days (dashed), 1 day (solid), and 0.5 day (dot–dashed) are shown. These curves demonstrate the effects of effect 2.

probability function versus intrinsic frequency for waves with vertical wavelength $\lambda_z = 2.5$ km, $\epsilon_0 = 0.2$, and $t_2 = 1$ day. It is clear from the shape of these probability functions that the group velocity effect will greatly emphasize low-frequency waves in observations. Parameter ϵ_0 in (7) might also have some dependence on $\hat{\omega}$ that, if present, would likely further enhance the low-frequency bias. Further, if the horizontal data sampling were sparse, and if observation points lay some distance from common source locations, then low-frequency waves with very large horizontal-to-vertical group velocity ratios might be additionally enhanced in observations because such waves can propagate farther horizontally from their sources before leaving the lower stratosphere. These effects will be neglected here, so we are assuming a sufficiently dense observation grid, and for lack of constraints, a constant ϵ_0. We have also chosen λ_z to match the peak energy in the spectrum observed in the lower stratosphere (Tsuda et al. 1994; Allen and Vincent 1995; Shimizu and Tsuda 1997; Tsuda et al. 1991). Such observations suggest little or no variation in the peak λ_z with latitude.

It is clear in Fig. 5 that the area under these curves has a latitudinal dependence. This is shown in Fig. 6 for three different intermittency periods $t_2 = 0.5$, 1, and 5 days. These latitudinal variations isolate the probability of observation effect. If every wave at any frequency were generated with the same amplitude temperature perturbation and same spatial and temporal intermittency at each latitude, these curves would describe the variation in $E_p(\phi)$ that would be observed. The effect never gives more than a 20% increase from 35° to 5°, and choosing other vertical wavelengths or values of ϵ_0 give similar results.

c. Combined effects

The calculations in Fig. 6 isolated only the group velocity effect. If waves at different frequencies are not generated with equal temperature amplitude and there is intermittency in the forcing, a different latitudinal dependence would result as a combination of the effects described in sections 3a and 3b.

Here we must take a moment to define what we will call a gravity wave source spectrum E_s and to distinguish that from the spectrum that can be observed E_o. The source spectrum E_s describes the distribution of wave energy generated by the source. Since the focus of this paper is on tropical and subtropical latitudes, the main source is likely convection. The spectrum E_s describes local gravity-wave amplitudes, information a gravity wave parameterization requires as input. The reason a distinction between E_o and E_s must be made is partly related to the diluting effects of averaging when dealing with intermittent phenomena, and partly due to the fact that gravity wave parameterizations neglect the propagation time effects related to wave vertical group velocity. Parameterizations make the simplifying assumption that the input waves instantaneously affect the column of atmosphere above.

The observable spectrum E_o is instead one that could be derived from a Lagrangian frame of reference such as from balloons floating on a constant pressure surface (Quinn and Holzworth 1987; Hertzog and Vial 2001) from which intrinsic frequency spectra can be derived. Here, E_o and E_s are related to one another via the probability of observation function described in section 3b and Eq. (7). The potential energy source spectrum is related to wave temperature amplitudes at the source $T'_s(\hat{\omega})$ via

$$E_s(\hat{\omega}) = \frac{1}{2}\left(\frac{g}{N}\right)^2\left[\frac{T'_s(\hat{\omega})}{\overline{T}}\right]^2\frac{1}{\Delta\hat{\omega}}, \qquad (8)$$

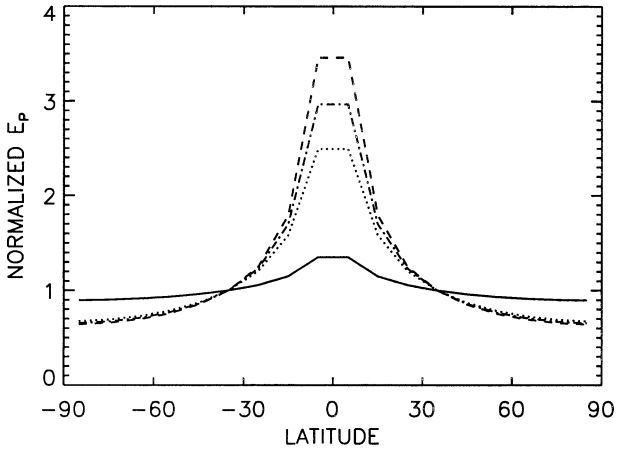

FIG. 7. Latitudinal variations in normalized variance allowing for both the effects of source intermittency and a source spectrum proportional to $\hat{\omega}^{-1}$. The intermittency varies in each curve: 2 days (dashed), 1 day (dash–dotted), 0.5 day (dotted), and no intermittency (solid). These curves demonstrate the combined effects of effects 1 and 2.

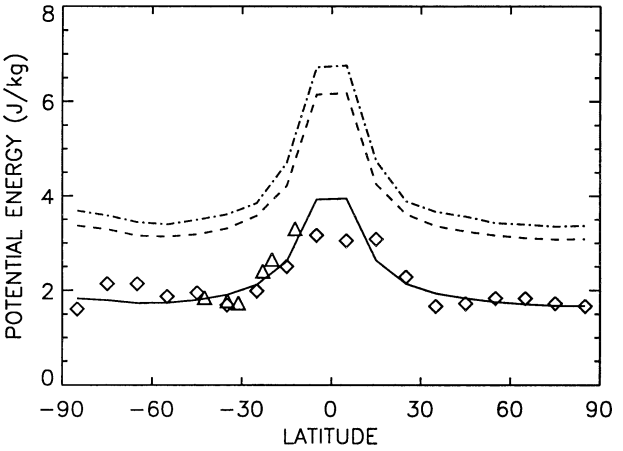

FIG. 8. Gravity-wave potential energy vs latitude. The symbols show the observations: Australian radiosondes (triangles), and GPS/MET observations (diamonds). The curves are model results with different parameters: $q = 1.3$ with no intermittency (dashed), $q = 0.7$ with 0.8-day intermittency (solid), and $q = 0.5$ with 2-day intermittency (dash–dotted). All three give the same ratio $E_p(5°)/E_p(35°) \sim 2$, but result in different total potential energies.

where $\overline{T}$ is background temperature and g is the gravitational acceleration. The observable spectrum E_o is then related to E_s via

$$E_o(\hat{\omega}) = E_s(\hat{\omega})P(\hat{\omega}). \tag{9}$$

Given the shapes of the functions $P(\hat{\omega})$ shown in Fig. 5, the observable spectrum would be identical to the source spectrum at very low $\hat{\omega}$ where $P = 1$, but E_o would be much more steeply sloped than E_s at higher $\hat{\omega}$. For midrange frequencies, $f \ll \hat{\omega} \ll N$, the group velocity $c_{gz} \sim \hat{\omega}/m$, so the probability defined in (7) is $P \propto \hat{\omega}^{-1}$. The group velocity effects embodied in P therefore steepen the observed spectrum compared to the source spectrum over a wide range of $\hat{\omega}$, and this implies that source spectra input to gravity-wave parameterizations should be flatter than commonly assumed. The observed potential energy as a function of latitude can be written as

$$E_p(\phi) = \int_{f(\phi)}^{N} E_s(\hat{\omega})P(\hat{\omega})\, d\hat{\omega}. \tag{10}$$

Figure 7 shows the normalized potential energy $E_p(\phi)$ assuming a source spectrum $E_s(\hat{\omega}) \propto \hat{\omega}^{-1}$ and four values of the intermittency period $t_2 = 0$, 0.5, 1, and 2 days. Including both effects together, both the frequency spectrum shape and the group velocity effect, give a larger low-latitude peak than either effect gives alone. This occurs because the probability functions (Fig. 5) weight the integral (10) toward low $\hat{\omega}$ where the latitudinal variations associated with f occur. For higher intermittency, the slope of E_o is steepened by P over a broader range of $\hat{\omega}$ ($P \to 1$ at lower $\hat{\omega}$).

In summary, the results in Figs. 4, 6, and 7 suggest the observed change in potential energy of a factor of ~2 from subtropical to low latitudes (Fig. 1) could be explained with several different combinations of the parameter t_2 and the slope q of the source spectrum

$$E_s \propto \hat{\omega}^{-q}. \tag{11}$$

The ambiguity in these different interpretations can be somewhat removed by applying constraints on the normalization of E_o. Constraints exist on temperature variance for ground-based periods in the 1- to 3-day-period range near the equator (Sato et al. 1994). Sato et al. (1997) have argued the waves in these observations to be minimally affected by Doppler shifting, such that $\omega \sim \hat{\omega}$ for these observations. Figure 7c of Sato et al. (1994) shows significant interannual variations associated with quasi-biennial oscillation (QBO) wind variations. The time-mean variance is ~2 K². The four-times-daily radiosonde observations near the equator at Nauru (Boehm and Verlinde 2000; Holton et al. 2001) suggest a value ~1.4 K² in this period range. To normalize the spectrum in Eq. (10), we therefore apply

$$\overline{T}^2\left(\frac{1}{2}\frac{g^2}{N^2}\right)^{-1} \int_{\omega_1}^{\omega_2} E_o(\hat{\omega})\, d\hat{\omega} \sim 1.7 \text{ K}^2, \tag{12}$$

where $\overline{T}$ is the annual-averaged temperature in the 18- to 25-km region and $\omega_1 = 2\pi$ (3 day)$^{-1}$ and $\omega_2 = 2\pi$ (1 day)$^{-1}$.

Figure 8 shows latitudinal potential energy distributions $E_p(\phi)$ that result from this normalization and several combinations of the parameters t_2 and q. For sources that are continuously generating waves ($t_2 = 0$, dashed curve), the potential energies are generally larger than the observations. The lowest values of potential energy occur for intermediate $t_2 \sim 0.5$ to 1 day and moderately shallow source spectrum slopes $E_s \propto \hat{\omega}^{-0.6}$ to $\hat{\omega}^{-0.7}$ (solid line). For very intermittent sources with very shallow

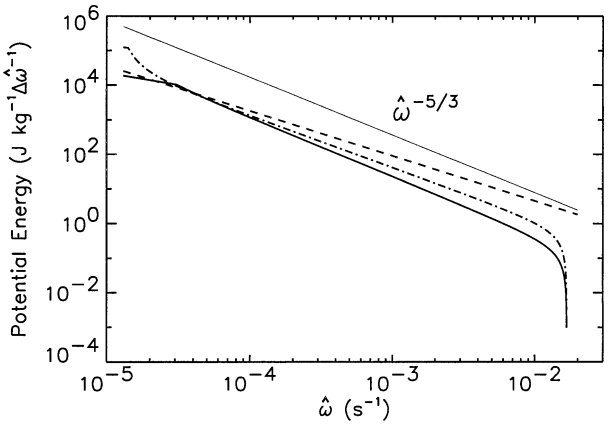

FIG. 9. Observable energy spectra $E_o(\hat{\omega})$ matching the three cases with the same parameter combinations and shown with the same line styles as the curves in Fig. 8: $q = 1.3$ with no intermittency (dashed), $q = 0.7$ with 0.8-day intermittency (thick solid), and $q = 0.5$ with 2-day intermittency (dash–dotted). The thin solid line shows a spectrum $\propto \hat{\omega}^{-5.3}$ for reference.

sloping E_s (dash–dotted curve) the potential energy is again larger because the normalization (12) applied at low frequencies boosts the wave amplitudes throughout the spectrum.

Each of the three curves in Fig. 8 also implies a different shape of the observable spectrum $E_o(\hat{\omega})$ calculation via (9) which are shown in Fig. 9 at 5° latitude. The intermediate case ($t_2 = 0.8$ day, $q = 0.7$, solid line) results in an observable spectrum with a shape $\sim\hat{\omega}^{-5/3}$ for periods shorter than about 35 h ($\hat{\omega} > 5 \times 10^{-5}$ s^{-1}). The spectra that include intermittency (solid and dot–dashed lines) also display steeper slopes at lower frequencies where the probability of observation $P \to 1$. These spectra then become quite flat where $P = 1$ because in this region of the spectrum $p = q$ and $E_o = E_s$. The spectrum also falls off steeply at very high $\hat{\omega}$ for the cases with intermittency near the buoyancy frequency N. The reason for this change is the term in the denominator of the group velocity (5) that involves N.

The normalization in (12) is rather uncertain, and the potential energies in Fig. 8 scale with this normalization factor. This uncertainty (in addition to the numerous simplifying assumptions made in these calculations) means we cannot derive any quantitative values for gravity-wave parameterization inputs from the observed latitudinal variations in gravity-wave potential energy with the information at hand. The above analysis, however, does provide some new perspectives on the interpretation of the observations that may allow subsequent studies to provide better constraints for gravity-wave parameterization inputs.

To underscore the importance of these group velocity effects to gravity-wave parameterization inputs, Fig. 10 shows momentum flux spectra that are consistent with the three cases discussed earlier: no intermittency ($t_2 = 0$ day, $p = 1.3$, dashed line); moderate intermittency ($t_2 = 0.8$ day, $q = 0.7$, solid line); and high intermittency ($t_2 = 2$ day, $q = 0.5$, dash–dotted line). Fritts and VanZandt (1993) give the theoretical conversion between potential energy and momentum flux. The curves in Fig. 10a (left panel) represent observable momentum flux spectra [derived from $E_o(\hat{\omega})$ thereby including the probability of observation effect]. The steepest of these is the moderate intermittency case for which the flux spectrum $\sim\hat{\omega}E_o(\hat{\omega}) \propto \hat{\omega}^{-0.7}$ for medium frequencies $f \ll \hat{\omega} \ll N$. For comparison, the constant pressure balloon data reported by Hertzog and Vial (2001) suggest a momentum flux spectrum $\sim\hat{\omega}^{-1}$ for frequencies higher than 2π 1 day^{-1}.

Momentum flux *source* spectra for these same three cases are shown in Fig. 10b. These would be the cor-

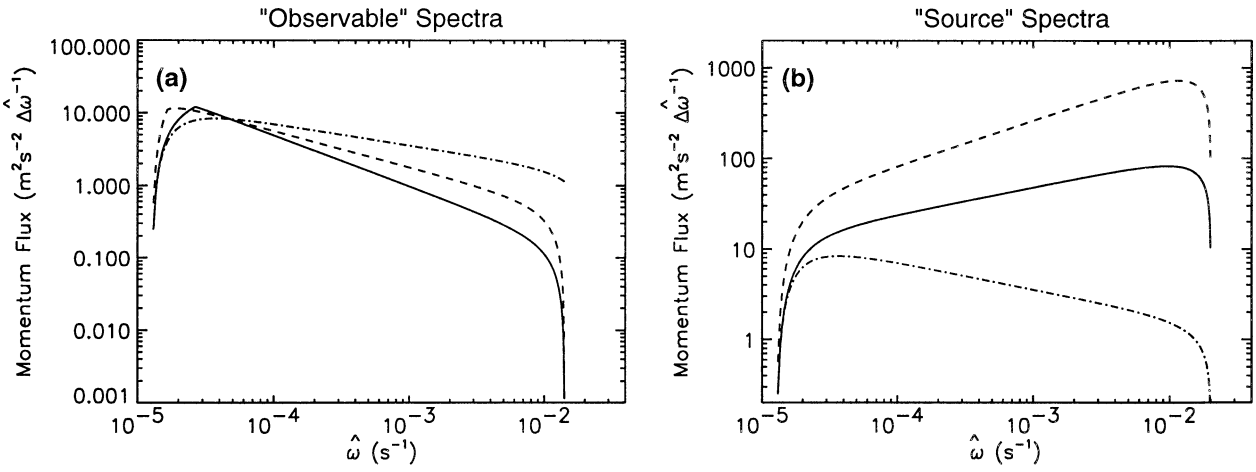

FIG. 10. (a) Observable momentum flux spectra vs intrinsic frequency matching the three cases with the same parameter combinations and shown with the same line styles as the curves in Figs. 8 and 9: $q = 1.3$ with no intermittency (dashed), $q = 0.7$ with 0.8-day intermittency (thick solid), and $q = 0.5$ with 2-day intermittency (dash–dotted). (b) Momentum flux spectra for the same cases as (a) but these are the associated spectra that would be appropriate for input to a GCM.

responding spectral shapes appropriate for input to a gravity-wave parameterization. The difference between the curves in Figs. 10a and 10b is the probability of observation $P(\hat{\omega}) \propto \hat{\omega}^{-1}$ for $f \ll \hat{\omega} \ll N$. The conclusion that follows is that when intermittency in the wave sources is considered in the interpretation of the observed momentum flux spectra, GCM parameterizations should input momentum flux spectra that are either flat or increase with intrinsic frequency, in contrast to traditional choices.

4. Summary and discussion

Knowledge of the latitudinal variations in the generation of gravity waves is important for their parameterization in global models. Observations of gravity waves with short vertical scales have shown a pronounced peak in wave activity at tropical latitudes (Fig. 1). In this paper, it is shown that such a peak would be a natural consequence of the latitudinal variation in the Coriolis parameter, which controls the lower limit for gravity-wave intrinsic frequencies (Fig. 2). Two distinct but related effects of this parameter on observations of gravity-wave activity are explained and explored with a simple model. The results are also compared to observed latitudinal variations in gravity-wave activity.

The results suggest that the intrinsic frequency spectrum of the wave sources E_s is likely much flatter than commonly assumed for source spectra input to gravity-wave parameterizations. Intermittency in gravity-wave forcing in the Tropics is also implied ($t_2 > 0$). The uncertainty in the normalization of the spectrum used in these calculations still leaves considerable uncertainty in the interpretation of the observations. Further, the model described here assumes no latitudinal variations in the shape of the wave spectrum or the intermittency. If these assumptions are incorrect we are left with an even greater uncertainty in the interpretation.

Additional constraints on intermittency must come from observations or models (e.g., Alexander 1996; Zink and Vincent 2001). Intermittency is also applied as a normalization in the Alexander and Dunkerton (1999) gravity-wave parameterization and is a potential rationale for the fudge factors applied in other parameterizations (Lindzen 1981; Holton 1982; Hines 1997). However, no consistent definition of this quantity exists. We hope the simple formulas presented in this paper may provide a first step toward defining intermittency, illustrating its role in relating gravity-wave parameterization inputs to observations, and stimulating new analyses of observations to help constrain it. Observational constraints from analyses such as Zink and Vincent (2001) using wavelet transform techniques to quantify intermittency are still difficult to interpret because the observations themselves are already biased towards observing low $\hat{\omega}$ waves by the group velocity effects described in the present paper. The necessary constraints may only come from better understanding of wave generation mechanisms so that by observing the wave sources themselves (e.g., latent heating in convection or cloud morphology) we may be able to quantify intermittency in wave forcing using models such as that in Bergman and Salby (1994).

The results also highlight that the observed latitudinal variations in short vertical wavelength waves only provide constraints on the low-frequency gravity waves with $\hat{\omega} \sim f - 4f$. Figure 5 suggests that the range of intrinsic frequencies observed should increase with decreasing latitude as $|f|$ decreases. This is a consequence of waves having intermittent sources. The dominance of low intrinsic frequencies in observations of short vertical wavelength waves is also consistent with observational analyses (Hirota 1984; Hamilton 1991; Eckermann et al. 1995; Vincent et al. 1997; Vincent and Alexander 2000; Alexander and Vincent 2000). Longer vertical wavelength and higher-frequency waves may have very different latitudinal variations (Wu and Waters 1996; Alexander 1998; McLandress et al. 2000). High-frequency waves certainly occur in the Tropics as evidenced by satellite observations (Dewan et al. 1998; McLandress et al. 2000); they are simply a small contributor to the short vertical wavelength signal in stratospheric temperature observations. The relative importance of high- and low-frequency waves to the net momentum flux carried vertically by tropical waves remains undetermined.

Figure 5 may also provide an interpretation of the frequency spectra shown in Sato et al. (1999) where a high-resolution GCM showed pronounced peaks near $\omega \sim f(\phi)$ at latitudes higher than $\sim 10^\circ$ and distributed over a broader range of ω at lower latitudes. Figure 5 shows this would be a natural result of the analysis if there were intermittency in the wave forcing in the model. The model analyzed by Sato et al. (1999) was an aquaplanet very high-resolution GCM, and one of the primary wave forcing mechanisms was convection.

Vincent et al. (1997) showed that low $\hat{\omega} < 2f$ waves were more likely to be observed in radiosonde data at Macquarie Island (55°S) than a model spectrum of gravity waves $E_o \propto \hat{\omega}^{-p}$ with $p = 5/3$ would predict, and Nastrom et al. (1997) describe a similar finding. The probability effects shown in Fig. 5 and associated spectra in Fig. 9 may explain these observed low $\hat{\omega}$ biases.

The observed peak in short vertical wavelength wave activity at low latitudes is not a direct indication of variations in gravity-wave sources as a function of latitude. The present work suggests that while there is likely an increase of net energy in gravity waves at low latitudes, the increases may be due only to a rather small increase in the creation of gravity-wave energy at low latitudes. (Note that larger energy at low latitudes could exist either because low-frequency waves are generated with larger amplitudes than the high-frequency waves, or equivalently because low-frequency-wave sources are less intermittent than high-frequency-wave sources. Either would give a time-averaged red spectrum.)

The model results shown here suggest that if relatively small increases in the creation of gravity-wave energy at low latitudes occurs preferentially at the lowest $\hat{\omega}$, then the observed gravity-wave energy at low latitudes will be enhanced by a much larger amount. The explanation is that low-frequency waves have slower vertical group velocities, so they will (all other things being equal) appear more frequently in the lower stratosphere than higher-frequency waves. Thompson (1978) put it this way: ''. . . once a packet of inertial waves is generated, it is in no hurry to leave the source region. Therefore, we expect to see waves with near-inertial period long after the higher-frequency waves have dispersed.''

Larger energies at low latitudes do not imply larger momentum fluxes. The low $\hat{\omega}$ waves likely carry much smaller momentum flux relative to higher $\hat{\omega}$ waves, so that in terms of momentum flux generated by sources as a function of latitude, the numbers may be smaller in the Tropics than at higher latitudes. This has implications for the relative fluxes at mid- and low latitudes assumed for parameterized gravity waves in studies such as Manzini and McFarlane (1998) and Scaife et al. (2000).

We note again that if any of the parameters assumed to be constant in latitude in this study instead vary with latitude, then different latitudinal variations in the modeled potential energy would result. The parameters that could have a large effect on the results are the values of the frequency spectrum exponent q, the intermittency period t_2, the spatial intermittency ϵ_0, and the spectral normalization. Because these parameters are not well-known, the results shown here can only be used to provide an interpretation of the low-latitude peak observed in gravity wave potential energy in a fairly qualitative sense.

5. Conclusions

There are four main conclusions we can draw.

1) We distinguish between observed intrinsic frequency spectra E_o and ''source spectra'' E_s. The latter is more relevant for constraining gravity wave parameterization input.
2) Over midrange frequencies $f \ll \hat{\omega} \ll N$, the source spectra have a greater dependence on high-frequency waves such that if $E_o \propto \hat{\omega}^{-p}$ then $E_s \propto \hat{\omega}^{1-p}$. This follows from the intrinsic frequency dependence of the vertical group velocity for fixed m and intermittency in wave forcing and is formalized here in a ''probability of observation'' function P.
3) The dependence of group velocity and P on intrinsic frequency may explain the low-frequency bias in stratospheric gravity-wave observations (Nastrom et al. 1997; Vincent et al. 1997).
4) The waves observed at low latitudes in Fig. 1 have low intrinsic frequencies with $\hat{\omega}$ near f. Because momentum flux $\sim \hat{\omega}E$, the low-latitude energy peak does not imply a corresponding low latitude peak in momentum flux.

Acknowledgments. The authors would like to thank Drs. Tim Dunkerton, Steve Eckermann, Dave Fritts, James Holton, and Kaoru Sato for their comments on the manuscript. This work was supported by grants from the National Science Foundation Physical Meteorology and Large-Scale Dynamic Meteorology Programs ATM-9907501, and POWRE Program 9870502. Robert A. Vincent thanks the Australian Research Council.

REFERENCES

Alexander, M., 1996: A simulated spectrum of convectively generated gravity waves: Propagation from the tropopause to the mesopause and effects on the middle atmosphere. *J. Geophys. Res.*, **101,** 1571–1588.

——, 1998: Interpretations of observed climatological patterns in stratospheric gravity wave variance. *J. Geophys. Res.,* **103,** 8627–8640.

——, and T. Dunkerton, 1999: A spectral parameterization of mean-flow forcing due to breaking gravity waves. *J. Atmos. Sci.,* **56,** 4167–4182.

——, and R. Vincent, 2000: Gravity waves in the tropical lower stratosphere: A model study of seasonal and interannual variability. *J. Geophys. Res.,* **105,** 17 983–17 993.

Allen, S., and R. Vincent, 1995: Gravity wave activity in the lower atmosphere: Seasonal and latitudinal variations. *J. Geophys. Res.*, **100,** 1327–1350.

Andrews, D., J. Holton, and C. Leovy, 1987: *Middle Atmosphere Dynamics.* Academic Press, 489 pp.

Bergman, J. W., and M. L. Salby, 1994: Equatorial wave activity derived from fluctuations in observed convection. *J. Atmos. Sci.,* **51,** 3791–3806.

Boehm, M., and J. Verlinde, 2000: Stratospheric influence on upper tropospheric tropical cirrus. *Geophys. Res. Lett.,* **27,** 3209–3212.

Dewan, E., and Coauthors, 1998: MSX satellite observations of thunderstorm-generated gravity waves in mid-wave infrared images of the upper stratosphere. *Geophys. Res. Lett.,* **25,** 939–942.

Eckermann, S., 1995: On the observed morphology of gravity-wave and equatorial-wave variance in the stratosphere. *J. Atmos. Terr. Phys.,* **57,** 105–134.

——, and P. Preusse, 1999: Global measurements of stratospheric mountain waves from space. *Science,* **286,** 1534–1537.

——, I. Hirota, and W. Hocking, 1995: Gravity wave and equatorial wave morphology of the stratosphere derived from long-term rocket soundings. *Quart. J. Roy. Meteor. Soc.,* **121,** 149–186.

Ecklund, W. L., K. S. Gage, G. D. Nastrom, and B. B. Balsley, 1986: A preliminary climatology of the spectrum of vertical velocity observed by clear-air doppler radar. *J. Climate Appl. Meteor.,* **25,** 885–892.

Fetzer, E. J., and J. C. Gille, 1994: Gravity wave variance in LIMS temperatures. Part I: Variability and comparison with background winds. *J. Atmos. Sci.,* **51,** 2461–2483.

——, and ——, 1996: Gravity wave variance in LIMS temperatures. Part II: Comparison with the zonal-mean momentum balance. *J. Atmos. Sci.,* **53,** 398–410.

Fritts, D., and T. VanZandt, 1987: Effects of doppler shifting on the frequency spectra of atmospheric gravity waves. *J. Geophys. Res.,* **92,** 9723–9732.

——, and ——, 1993: Spectral estimates of gravity wave energy and momentum fluxes. Part I: Energy dissipation, acceleration, and constraints. *J. Atmos. Sci.,* **50,** 3685–3694.

——, T. Tsuda, T. VanZandt, S. Smith, T. Sato, S. Fukao, and S. Kato, 1990: Studies of velocity fluctuations in the lower atmosphere using the MU radar. Part II: Momentum fluxes and energy densities. *J. Atmos. Sci.,* **47,** 51–66.

Hamilton, K., 1991: Climatological statistics of stratospheric inertia-gravity waves deduced from historical rocketsonde wind and temperature data. *J. Geophys. Res.,* **96,** 20 831–20 839.

Hertzog, A., and F. Vial, 2001: A study of the dynamics of the equatorial lower stratosphere by use of ultra-long duration balloons. Part II: Gravity waves. *J. Geophys. Res.* **106,** 22 745–22 761.

Hines, C., 1997: Doppler-spread parameterization of gravity-wave momentum deposition in the middle atmosphere. 1. Basic formulation. *J. Atmos. Solar-Terr. Phys.,* **59,** 371–386.

Hirota, I., 1984: Climatology of gravity waves in the middle atmosphere. *J. Atmos. Terr. Phys.,* **46,** 767–773.

Holton, J., 1982: The role of gravity wave induced drag and diffusion in the momentum budget of the mesosphere. *J. Atmos. Sci.,* **39,** 791–799.

——, M. Alexander, and M. Boehm, 2001: Evidence for short vertical wavelength Kelvin waves in the DOE-ARM Nauru99 radiosonde data. *J. Geophys. Res.* **106,** 20 125–20 129.

Kinnersley, J., 1996: The climatology of the stratospheric ''thin air'' model. *Quart. J. Roy. Meteor. Soc.,* **122,** 219–252.

Kitamura, Y., and I. Hirota, 1989: Small-scale disturbances in the lower stratosphere revealed by daily rawin sonde observations. *J. Meteor. Soc. Japan,* **67,** 817–830.

Lindzen, R. S., 1981: Turbulence and stress owing to gravity wave and tidal breakdown. *J. Geophys. Res.,* **86,** 9707–9714.

Manzini, E., and N. McFarlane, 1998: The effect of varying the source spectrum of a gravity wave parameterization in a middle atmosphere general circulation model. *J. Geophys. Res.,* **103,** 31 523–31 539.

McFarlane, N. A., 1987: The effect of orographically excited gravity wave drag on the general circulation of the lower stratosphere and troposphere. *J. Atmos. Sci.,* **44,** 1775–1800.

McLandress, C., M. J. Alexander, and D. Wu, 2000: Microwave limb sounder observations of gravity waves in the stratosphere: A climatology and interpretation. *J. Geophys. Res.,* **105,** 11 947–11 967.

Medvedev, A., G. Klaassen, and S. Beagley, 1998: On the role of an anisotropic gravity wave spectrum in maintaining the circulation of the middle atmosphere. *Geophys. Res. Lett.,* **25,** 509–512.

Nastrom, G., T. VanZandt, and J. Warnock, 1997: Vertical wavenumber spectra of wind and temperature from high-resolution balloon soundings in the lower atmosphere over Illinois. *J. Geophys. Res.,* **102,** 6685–6702.

Ogino, S., M. Yamanaka, and S. Fukao, 1995: Meridional variation of lower stratospheric gravity wave activity: A quick look at Hakuho-maru J-COARE cruise rawinsonde data. *J. Meteor. Soc. Japan,* **73,** 407–413.

Pfister, L., W. Starr, R. Craig, and M. Loewenstein, 1986: Small-scale motions observed by aircraft in the tropical lower stratosphere: Evidence for mixing and its relationship to large-scale flows. *J. Atmos. Sci.,* **43,** 3210–3225.

Preusse, P., S. Eckermann, and D. Offermann, 2000: Comparison of global distributions of zonal-mean gravity wave variance inferred from different satellite instruments. *Geophys. Res. Lett.,* **27,** 3877–3880.

Quinn, E., and R. Holzworth, 1987: Quasi-lagrangian measurements of density surface fluctuations and power spectra in the stratosphere. *J. Geophys. Res.,* **92,** 10 926–10 932.

Rind, D., R. Suozzo, and N. K. Balachandran, 1988: The GISS Global Climate–Middle Atmosphere Model. Part II: Model variability due to interactions between planetary waves, the mean circulation and gravity wave drag. *J. Atmos. Sci.,* **45,** 371–386.

Sato, K., 1990: Vertical wind disturbances in the troposphere and lower stratosphere observed by the MU radar. *J. Atmos. Sci.,* **47,** 2803–2817.

——, F. Hasegawa, and I. Hirota, 1994: Short-period disturbances in the equatorial lower stratosphere. *J. Meteor. Soc. Japan,* **72,** 859–872.

——, D. O'Sullivan, and T. Dunkerton, 1997: Low-frequency inertia-gravity waves in the stratosphere revealed by three-week continuous observation with the MU radar. *Geophys. Res. Lett.,* **24,** 1739–1742.

——, T. Kumakura, and M. Takahashi, 1999: Gravity waves appearing in a high-resolution GCM simulation. *J. Atmos. Sci.,* **56,** 1005–1018.

Scaife, A., N. Butchart, C. Warner, D. Stainforth, and W. Norton, 2000: Realistic quasi-biennial oscillations in a simulation of the global climate. *Geophys. Res. Lett.,* **27,** 3481–3484.

Shimizu, A., and T. Tsuda, 1997: Characteristics of Kelvin waves and gravity waves observed with radiosondes over Indonesia. *J. Geophys. Res.,* **102,** 26 159–26 171.

Thompson, R., 1978: Observation of inertial waves in the stratosphere. *Quart. J. Roy. Meteor. Soc.,* **104,** 691–698.

Tsuda, T., T. VanZandt, M. Mizumoto, S. Kato, and S. Fukao, 1991: Spectral analysis of temperature and Brunt-Väisälä frequency fluctuations observed by radiosondes. *J. Geophys. Res.,* **96,** 17 265–17 278.

——, Y. Murayama, H. Wiryosumarto, S. W. B. Harijono, and S. Kato, 1994: Radiosonde observations of equatorial atmosphere dynamics over Indonesia. 2. characteristics of gravity waves. *J. Geophys. Res.,* **99,** 10 507–10 516.

——, M. Nishida, C. Rocken, and R. H. Ware, 2000: A global morphology of gravity wave activity in the stratosphere revealed by the GPS occultation data (GPS/MET). *J. Geophys. Res.,* **105,** 7257–7274.

Vincent, R., and M. Alexander, 2000: Gravity waves in the tropical lower stratosphere: An observational study of seasonal and interannual variability. *J. Geophys. Res.,* **105,** 17 971–17 982.

——, S. Allen, and S. Eckermann, 1997: Gravity-wave parameters in the lower stratosphere. *Gravity Wave Processes and Their Parameterization in Global Climate Models,* K. Hamilton, Ed., Springer-Verlag, 7–25.

Warner, C., and M. McIntyre, 1996: On the propagation and dissipation of gravity wave spectra through a realistic middle atmosphere. *J. Atmos. Sci.,* **53,** 3213–3235.

——, and ——, 2001: An ultrasimple spectral parameterization for nonorographic gravity waves. *J. Atmos. Sci.,* **58,** 1837–1857.

Wu, D., and J. Waters, 1996: Gravity-wave-scale temperature fluctuations seen by the UARS MLS. *Geophys. Res. Lett.,* **23,** 3289–3292.

Zink, F., and R. Vincent, 2001: Wavelet analysis of stratospheric gravity wave packets over Macquarie Island. Part II: Intermittency and mean-flow accelerations. *J. Geophys. Res.,* **106,** 10 289–10 297.